Int. J. Electrochem. Sci., 14 **(2019)** 1500 – 1515, doi: 10.20964/2019.02.55

International Journal of ELECTROCHEMICAL SCIENCE
www.electrochemsci.org

Synthesis and Structure of New Mixed Silver Cobalt(II)/(III) Diphosphate - $Ag_{3.68}Co_2(P_2O_7)_2$. Silver(I) Transport in the Crystal

Mohamed Amine Ben Moussa[1], *Riadh Marzouki*[2,*], *Ameni Brahmia*[2,3], *Samuel Georges*[4], *Saïd Obbade*[4], *Mohamed Faouzi Zid*[1]

[1] Laboratory of Materials, Crystallochemistry and Applied Thermodynamics, Faculty of Sciences of Tunis, University of Tunis El Manar, Tunisia.
[2] Chemistry Department, College of Science, King Khalid University, Abha 61413, Saudi Arabia.
[3] Materials Chemistry and the Environment Research Unit, University of Tunis El Manar, 2092 Tunis, Tunisia.
[4] CNRS, LEPMI, F-38000 Grenoble, France.
[*]E-mail: riadh.marzouki@hotmail.fr

Received: 3 October 2018 / *Accepted:* 5 November 2018 / *Published:* 5 January 2019

A new silver cobalt diphosphate, $Ag_{3.68}Co_2(P_2O_7)_2$, is synthesized by solid-state reaction route. Crystal structure and Ag^+ pathways simulation are studied by single-crystal X-ray diffraction and Bond Valence Site Energy (BVSE) model, respectively. The title material crystallizes in the triclinic system, space group P-1 with a = 6.521(4) Å, b = 9.623(6) Å, c = 10.969(7) Å, α = 64.23(2)˚, β = 80.14(3)˚ and γ = 72.10(2)˚. The structure presents $Co_4P_4O_{28}$ groups formed by two Co_2O_{11} units and two P_2O_7 groups. The junction between these groups is assured by two pyrophosphates to create a three-dimensional anionic framework showing interconnecting tunnels in *a*, *b* and *c* axis. The obtained structural model is supported by two validations tools: Charge Distribution (CHARDIT) analysis and Bond Valence Sum (BVS) calculation which validated the presence of Co^{2+} and Co^{3+} in the same sites. The Ag^+ cations balanced the negative charge with partial site occupations. The Ag^+ pathways simulation, using the Bond Valence Site Energy (BVSE) model, identified the mobile species and proposed migration pathways of the monovalent cations according vast tunnels in three dimensions. The material must be a 3D average ionic conductor, with theoretical activation energy about 1.7 eV. Correlation between structure and electrical properties has been discussed.

Keywords: diphosphate, structure, tunnels, pathways simulation, ionic conductor.

1. INTRODUCTION

Investigation of inorganic materials with open frameworks formed by tetrahedra, pentahedra or/and octahedra sharing faces, edges and/or corners, demarcating cages, inter-layer spaces or tunnels

where cations are located, is currently an intense activity field spanning several disciplines chiefly solid state chemistry. Particularly, the monovalent (Li; Na; K; Ag) and transition metals phosphates show a promising field for various applications: electrical, magnetic, optical, ferroelectric, etc [1-6]. In fact, It presents remarkable structural richness, particularly the melilite structure [6-8], the olivine structure [9] and the NaSICON (Sodium Super Ionic Conductor) structure [10], these materials have numerous physical properties such as ionic conduction and ion exchange [9, 12]. Recently, several studies have been devoted to the investigation of monovalent cation cobalt diphosphates due to their interesting physical properties. In fact, It shows a remarkable electrical and magnetic properties same as in the $Na_2CoP_2O_7$ [13] and $K_2CoP_2O_7$ [8].

This work is dedicated to the investigation of new silver cobalt (+II/+III) diphosphate synthesized by solid state route. The crystal structure of the title material is characterized via X-ray diffraction. BVS and CHARDIT tools are used to confirm the occupancy rate of Co^{2+} and Co^{3+} in the same sites. The BVSE model calculations allowed defining theoretically the electrical behavior of the studied material.

2. EXPERIMENTAL

2.1. Synthesis of $Ag_{3.68}Co_2(P_2O_7)_2$

$Ag_{3.68}Co_2(P_2O_7)_2$ was synthesized by solid state reaction. In fact, high-purity reagents $AgNO_3$ (99.5%, Fluka), $Co(NO_3)_2.6H_2O$ (99%, Aldrich) and $NH_4H_2PO_4$ (≥ 99%, Fluka) with Ag:Co:P molar ratio of 2:1:2 are dissolved in aqueous solution. After slowly evaporation at 120°C, the obtained residue is placed in porcelain crucible and heated at 350 °C for 12 hours. Thereafter, the mixture was progressively annealed at 610°C for 3 days. Finally, it was slowly cooled down at $2°C.h^{-1}$ to room temperature. Purple crystals of the title material were separated by boiling water washing. A single crystal was isolated for structural analysis by X-ray diffraction.

2.2. Characterizations

A single crystal specimen of the title material, approximate dimensions 0.24×0.13×0.11 mm^3, was selected for the X-ray crystallographic analysis. The X-ray intensity data were measured. The data were collected on a Kappa-CCD Apex diffractometer using the MoKα (λ=0.71069Å) radiation at room temperature. Data were corrected for absorption effects using the Numerical Mu From Formula method (SADABS) [14]. The ratio of minimum to maximum apparent transmission was 0.713. The calculated minimum and maximum transmission coefficients (based on crystal size) are 0.2190 and 0.4400.

All subsequent calculations were carried out using the SHELX-97 [15] computer programs included in the WinGX software package [16]. Structure graphics were drawn with Diamond 2.1 program [17]. A summary of the fundamental crystal data is given in Table 1.

Table 1. Crystal data refinement results of $Ag_{3.68}Co_2(P_2O_7)_2$

Crystallographic data	
Empirical formula	$Ag_{3.68}Co_2(P_2O_7)_2$
Crystal system; Space group	Triclinic; $P\bar{1}$
Unit cell dimensions	a = 6.521(4) Å ; α = 64.23(2)° b = 9.623(6) Å ; β = 80.14(3)° c = 10.969(7) Å ; γ = 72.10(2)°
Formula weight; Density ρ_{cal}	862.70 $gmol^{-1}$; 5.056 g/cm^3
Wavelength; Temperature	0.71073 Å; 296(2) (K)
Crystal size (mm)	0.24 × 0.13 × 0.11
Color; Crystal form	Pink; Parallelepiped
V ($Å^3$); Z	589.37(6); 2
Absorption coefficient μ; F (000)	9.89 mm^{-1}; 828
Data collection	
Scan mode	ω-2θ
Data collection range Range of indices	3.29°≤ θ ≤ 34.47° -10≤ h ≤ 10 -14≤ k ≤ 15 -17≤ l ≤ 17
Reflections measured	52741
T_{min} ; T_{max}	0.2036; 0.4203
Reference rays	-3 2 -6 ; -3 1 -6
Deviation; Exposure time	1.1%; 19.09 hours
Refinement	
Refinement method	Full-matrix least-squares on F^2
Final R indices [I> 2σ(I)]	R(F)=0.024; wR(F^2)=0.057
Independent Reflections; parameters	4620; 258
Extinction coefficient	0.0012(2)
Goodness of fit	1.08

2.3. Computational method: Bond Valence Energy Model:

The concept of bond valence [18,19] commonly used to validate the plausibility of crystal structure determination such as in $Na_4Li_{0.62}Co_{5.67}Al_{0.71}(AsO_4)_6$ [20], $Na_4Co_{5.63}Al_{0.91}(AsO_4)_6$ [21], $Na_9Cr(MoO_4)_6$ [22] . On the other hand, It was successfully involved to simulate sodium ion pathways

in several materials such as $Na_4Co_{5.63}Al_{0.91}(AsO_4)_6$ [23], $Na_4Co_7(AsO_4)_6$ [24], $NaCo_2As_3O_{10}$ arsenates [25] and $Na_2Co_2(MoO_4)_3$ molybdate [26]. While bond valences $s_{A\text{-}X} = exp\ [(R_0 - R_{A\text{-}X}) / b]$ for the interaction between a cation (A) and an anion (X) as well as their mismatches are mostly expressed in arbitrary "valence units", they may shown recently also be linked to an absolute energy scale by expressing the bond valence as a Morse-type interaction energy [27-28]. In brief, the pathway approach identifies regions of low site energy $E(A)$

$$E(\mathrm{A}) = D_0\left[\sum_{i=1}^{N}\left(\frac{s_{\mathrm{A-X_i}} - s_{\mathrm{min,A-X}_i}}{s_{\mathrm{min,,A-X_i}}}\right)^2 - N\right] + E_{\mathrm{Coulomb}}(\mathrm{A-B}) \qquad (1)$$

as regions that the mobile cation A can reach with an activation energy related to the value of $E(A)$. For the purpose of such a transport pathway analysis by means of bond-valence site energy landscapes, it has proven useful to consider among the Coulomb repulsions of the mobile cation only those with the immobile cation types B so that collective motions of mobile ions can be captured. In both cases Coulomb repulsions are screened by an error function complement term

$$E_{Coulomb}(A-B) = 14.4\frac{eV}{\mathring{A}}\frac{z_A \cdot z_B}{R_{A-B}}erfc\left(\frac{R_{A-B}}{\rho_0}\right) \qquad (2)$$

and the fractional ion charges z_A, z_B are derived from the nominal charges and principal quantum numbers by the formalism explained in [27,28]. Coulomb attraction terms are generally integrated in the Morse attraction term.

3. RESULTS AND DISCUSSION

3.1. Structure refinement and validation:

The structure was treated by direct methods via SHELXS-97 program [15]. In fact, in the closest solution proposed by program, some atoms of silver, cobalt and phosphor were located. Using SHELXL-97 program [15], refinements followed by Fourier differences are necessary to find the positions of others atoms with total occupations remaining in the lattice to an R factor of 5.3% for all reflections. In this case, high thermal agitation of the silver cations is noticed. Refinement of Ag elements occupancies was conducted and showed fractional occupancy for all positions of silver. The values of thermal agitation are then acceptable with the partial occupations. The obtained formula is $Ag_{3.68}Co_2(P_2O_7)_2$ with reliability factor R=2.4%. However, the electroneutrality is not ensured with Ag^+, Co^{2+}, P^{5+} and O^{2-} ions. Three hypotheses are then possible. The first one is the presence of another element with higher oxidation number in the same Co^{2+} sites which has been encountered in previous studies, such as Al^{3+} in $Na_4Li_{0.62}Co_{5.67}Al_{0.71}(AsO_4)_6$ [20] and $Na_4Co_{5.63}Al_{0.91}(AsO_4)_6$ [21] materials. The second hypothesis is the existence of some vacancies in the Oxygen element sites such as in $SrCo_{0.85}Fe_{0.15}O_{2.62}$ [29]. The third proposition is the oxidation of an amount of Co^{2+}. For that, qualitative analysis using Electron dispersion spectroscopy EDS was performed. It shows that no additional elements are presented in the studied sample. Thereby, the first hypothesis is excluded. In a second step, a refinement of O elements occupancies was conducted and did not show any deviation from full occupancy. So, the second hypothesis was also excluded. Then, the third proposition will

then be retained. The oxidation number of transition metals M^{+2}/M^{3+} in the same site has been encountered in previous work, especially in the same family of the studied diphosphate including: $Na_{3.5}Mg_{2.25}(P_2O_7)_2$ [30], $Na_{3.12}Fe_{2.44}(P_2O_7)_2$ [31], $Na_{3.64}Mg_{2.18}(P_2O_7)_2$ and $Na_{3.64}Ni_{2.18}(P_2O_7)_2$ [32]. In our case, it remains to determine the Co^{2+} and Co^{3+} occupations in each site. For it, the obtained structural model is supported by BVS [18,19] and CHARDI [33,34] validation tools where V and Q present the valences and the computed charge calculated by BVS model and CHARDI analysis, respectively. The obtained values are summarized in table 2. The results show that valences and charges values of cobalt are relatively higher than +2. Indeed, Co1 and Co2 charge values are +2.121 and +2.197, respectively. It shows the existence of a proportion of Co^{3+} in both sites. Based on the results found, the sites occupations must be Co1 = ($0.88Co^{2+}$ / $0.12Co^{3+}$) and Co2 = ($0.80Co^{2+}$ / $0.20Co^{3+}$). From where, the formula of the studied compound is $Ag_{3.68}(Co^{II}_{1.68}Co^{III}_{0.32})(P_2O_7)_2$. The electroneutrality is then ensured.

Table 2. CHARDI and BVS analysis of cation polyhedra in $Ag_{3.68}Co_2(P_2O_7)_2$:

Cation	V	q.sof	Q	CN	ECoN
Co1	2.111	2.120	2.121	6	5.93
Co2	2.191	2.20	2.197	6	5.91
P1	4.982	5.00	5.054	4	3.98
P2	4.994	5.00	4.923	4	3.99
P3	4.989	5.00	4.991	4	3.98
P4	4.942	5.00	5.049	4	3.97

Co1=$0.88Co^{2+}$ / $0.12Co^{3+}$; Co2 = $0.80Co^{2+}$ / $0.20Co^{3+}$

q(i) = formal oxidation number; sof(i) = site occupation factor; Q(i) = calculated charge

CN = coordination number; ECoN = Effective coordination number

Atomic positions and isotropic thermal factor of $Ag_{3.68}Co_2(P_2O_7)_2$ are collected in table 3.

Table 3. Atomic positions and isotropic thermal factor of $Ag_{3.68}Co_2(P_2O_7)_2$

Atoms	x	y	z	U_{iso}*/U_{eq}	*Occ. (<1)*
Co1	0.64967 (5)	0.26890 (4)	0.23860 (3)	0.00812 (7)	
Co2	0.28927 (6)	0.38367 (4)	0.72155 (3)	0.00869 (7)	
Ag1	0.2081 (10)	0.4376 (3)	0.4096 (6)	0.0259 (5)	0.60
Ag11	0.2356 (8)	0.4654 (10)	0.3801 (4)	0.0259 (5)	0.15
Ag13	0.215 (2)	0.4151 (13)	0.4180 (17)	0.0259 (5)	0.25
Ag2	0.3583 (8)	0.9932 (7)	0.1456 (7)	0.0325 (7)	0.29
Ag22	0.3944 (12)	0.0023 (7)	0.1694 (6)	0.0325 (7)	0.19
Ag23	0.3984 (7)	0.9889 (4)	0.1530 (3)	0.0414 (6)	0.52
Ag3	0.03551 (5)	0.79188 (4)	0.03216 (3)	0.02296 (10)	0.8042 (15)
Ag4	0.733 (2)	0.9545 (5)	0.5584 (4)	0.0340 (12)	0.34 (2)

Ag41	0.522 (9)	0.993 (5)	0.5159 (19)	0.062 (10)	0.074 (2)
Ag42	0.6883 (10)	0.9553 (4)	0.5597 (3)	0.0352 (7)	0.47 (2)
P1	0.57705 (10)	0.65185 (7)	0.03974 (6)	0.00712 (11)	
P2	0.28358 (10)	0.72680 (8)	0.45951 (6)	0.00833 (11)	
P3	0.88146 (10)	0.63474 (8)	0.81404 (6)	0.00775 (11)	
P4	0.90611 (11)	0.89283 (8)	0.29166 (7)	0.01019 (12)	
O1	0.3145 (3)	0.2711 (3)	0.2752 (2)	0.0145 (4)	
O2	0.2330 (4)	0.5663 (2)	0.5331 (2)	0.0146 (4)	
O3	0.1391 (4)	0.2678 (3)	0.6642 (2)	0.0186 (4)	
O4	0.9753 (3)	0.2616 (2)	0.2021 (2)	0.0164 (4)	
O5	0.3709 (3)	0.2119 (2)	0.9447 (2)	0.0140 (4)	
O6	0.0076 (3)	0.5189 (2)	0.2044 (2)	0.0134 (3)	
O7	0.7090 (3)	0.0205 (2)	0.3057 (2)	0.0143 (4)	
O8	0.5779 (3)	0.2601 (3)	0.6690 (2)	0.0154 (4)	
O9	0.5667 (3)	0.5205 (2)	0.18215 (18)	0.0101 (3)	
O10	0.6148 (3)	0.2962 (2)	0.04319 (19)	0.0134 (3)	
O11	0.0269 (4)	0.9447 (3)	0.1567 (2)	0.0223 (4)	
O12	0.0609 (3)	0.8632 (2)	0.40863 (19)	0.0111 (3)	
O13	0.6316 (3)	0.2280 (2)	0.4464 (2)	0.0138 (4)	
O14	0.7837 (3)	0.5749 (2)	0.96591 (18)	0.0110 (3)	

3.2. Crystal structure:

The summary of the recording conditions and structure refinement results of the title material are collected in Table 1. Table 3 contains the atomic coordinates and isotropic thermal factors. The main interatomic distances in coordination polyhedra of the studied structure are presented in Table 4.

Table 4. Interatomic distances in coordination polyhedra in $Ag_{3.68}Co_2(P_2O_7)_2$

Co1—O4	2.078 (2)	Co2—O3	2.022 (2)
Co1—O10	2.0871 (19)	Co2—O8	2.035 (2)
Co1—O7	2.098 (2)	Co2—O2	2.050 (2)
Co1—O13	2.126 (2)	Co2—O6^{ii}	2.0722 (19)
Co1—O9	2.1314 (19)	Co2—O9^{i}	2.1374 (19)
Co1—O1	2.149 (2)	Co2—O5	2.322 (2)
P1—O10^{ix}	1.501 (2)	P2—O2	1.511 (2)
P1—O9	1.5306 (19)	P2—O13^{i}	1.515 (2)
P1—O5^{i}	1.534 (2)	P2—O8^{i}	1.516 (2)
P1—O14^{vii}	1.598 (2)	P2—O12	1.616 (2)

P3—O4^{xi}	1.504 (2)	P4—O11^{xii}	1.504 (2)
P3—O6^{i}	1.518 (2)	P4—O3^{i}	1.514 (2)
P3—O1^{i}	1.535 (2)	P4—O7^{x}	1.520 (2)
P3—O14	1.5941 (19)	P4—O12^{xii}	1.641 (2)
Ag13—O1	2.404 (9)	Ag2—O5^{iii}	2.303 (6)
Ag13—O3	2.489 (19)	Ag2—O11	2.321 (5)
Ag13—O6	2.558 (10)	Ag2—O8^{i}	2.368 (6)
Ag11—O6	2.416 (4)	Ag22—O8^{vi}	2.343 (6)
Ag11—O1	2.482 (7)	Ag22—O5^{vii}	2.405 (6)
Ag13—O2	2.340 (8)	Ag23—O8^{i}	2.321 (4)
Ag3—O10^{ix}	2.319 (2)	Ag23—O5^{iii}	2.345 (4)
Ag3—O11	2.388 (2)	Ag23—O5^{i}	2.571 (4)
Ag3—O11^{iv}	2.444 (2)	Ag23—O11	2.576 (5)
Ag3—O6	2.523 (2)	Ag4—O1^{i}	2.217 (6)
Ag4—O7^{x}	2.583 (4)	Ag41—O7^{i}	2.24 (4)
Ag4—O13^{x}	2.295 (5)	Ag41—O13^{x}	2.35 (3)
Ag42—O1^{i}	2.148 (4)	Ag41—O7^{x}	2.36 (3)
Ag42—O13^{x}	2.300 (4)	Ag41—O13^{i}	2.47 (3)
Ag42—O7^{x}	2.565 (4)		

Symmetry codes: (i) −x+1, −y+1, −z+1; (ii) −x, −y+1, −z+1; (iii) x, y+1, z−1; (iv) −x, −y+2, −z; (v) −x+1, −y+2, −z; (vi) −x+1, −y, −z+1; (vii) x, y, z−1; (viii) −x+1, −y+2, −z+1; (ix) −x+1, −y+1, −z; (x) x, y+1, z; (xi) −x+2, −y+1, −z+1; (xii) x+1, y, z; (xiii) x, y−1, z+1; (xiv) x, y, z+1; (xv) x, y−1, z; (xvi) x−1, y, z.

The title diphosphate can be added to isostructural phases family including $Na_{2.84}Ag_{1.16}Co_2(P_2O_7)_2$ [35], $Na_{3.5}Mg_{2.25}(P_2O_7)_2$ [30], $Na_2CoP_2O_7$ [6], $Na_{3.12}Fe_{2.44}(P_2O_7)_2$ [31], $Na_{3.64}Mg_{2.18}(P_2O_7)_2$ and $Na_{3.64}Ni_{2.18}(P_2O_7)_2$ [32]. Except the $Na_2CoP_2O_7$ material, the others have a centrosymmetric structure. In fact, it crystallizes in the P-1 space group. On the other hand, the structure of sodium cobalt diphosphate is to claim to be not centrosymmetric (Space Group: P1) due to the deviation of sodium from a special position.

The environment of the asymmetric unit of $Ag_{3.68}Co_2(P_2O_7)_2$ is shown in figure 1. It shows a classic $Co(1)P_2O_{12}$ dimers formed by CoO_6 octahedron and sharing corner with P_2O_7. In the other side, a second CoO_6 octahedron connected by edge with a diphosphate forming $Co(2)P_2O_{11}$ group. The connection between CoP_2O_{11} and CoP_2O_{12} dimers is assured by two mixed bridges Co1–O9–P1 and Co2–O2–P2. The compensation charge is insured by the Ag^+ cations.

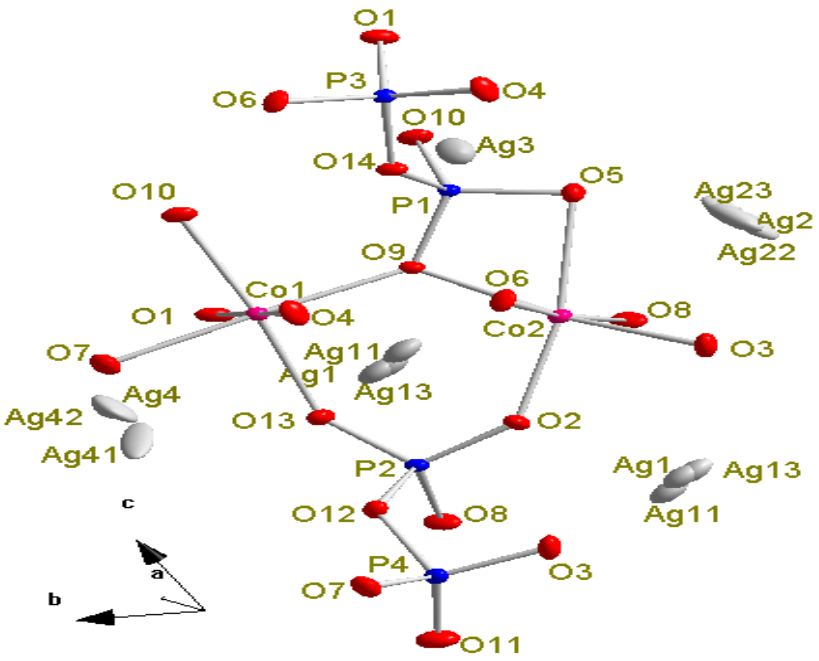

Figure 1. Environment of the asymmetric unit of $Ag_{3.68}Co_2(P_2O_7)_2$ compound

In the anionic framework, the cohesion between two symmetrical units $Co(2)P_2O_{11}$ (Fig. 2) is provided by $Co(1)O_6$ octahedra to form the $Co_4P_4O_{28}$ unit (Fig. 3). According the three spatial directions, the junction between two $Co_4P_4O_{28}$ units is provided by two P_2O_7 diphosphates forming 3D anionic framework.

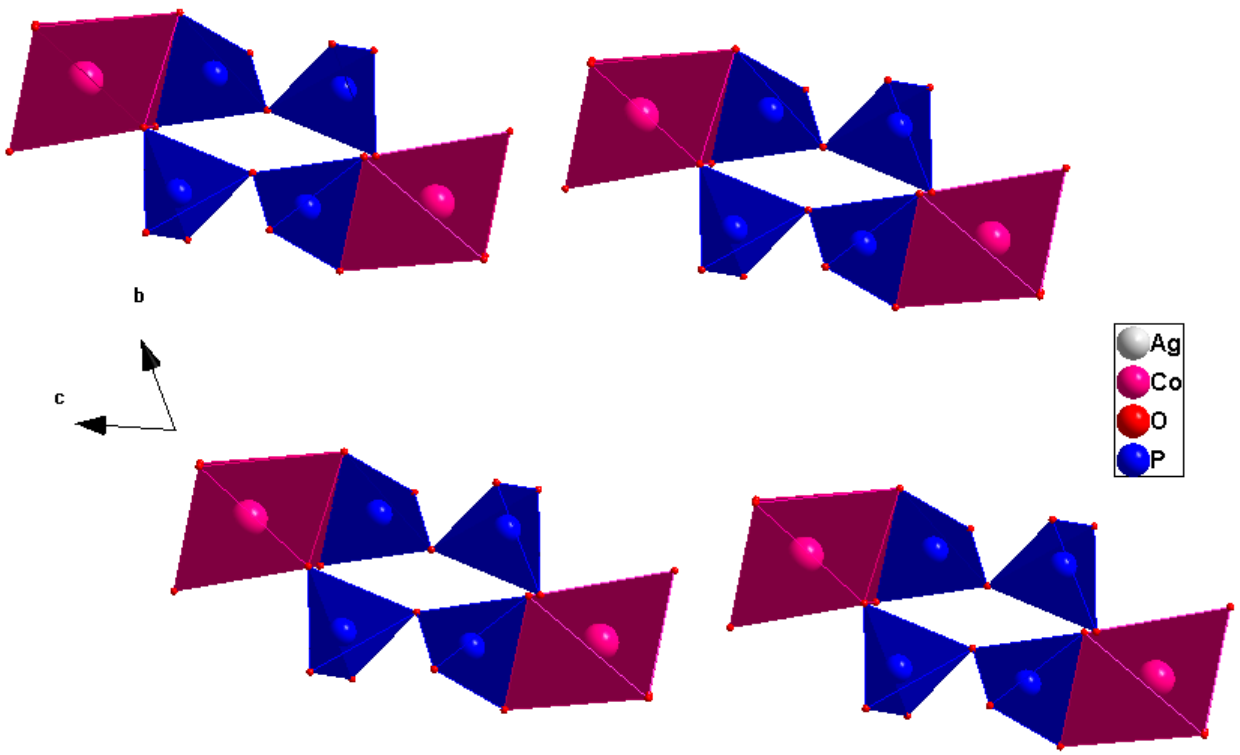

Figure 2. Arrangement of CoP_2O_{11} dimers projected in the [100] direction

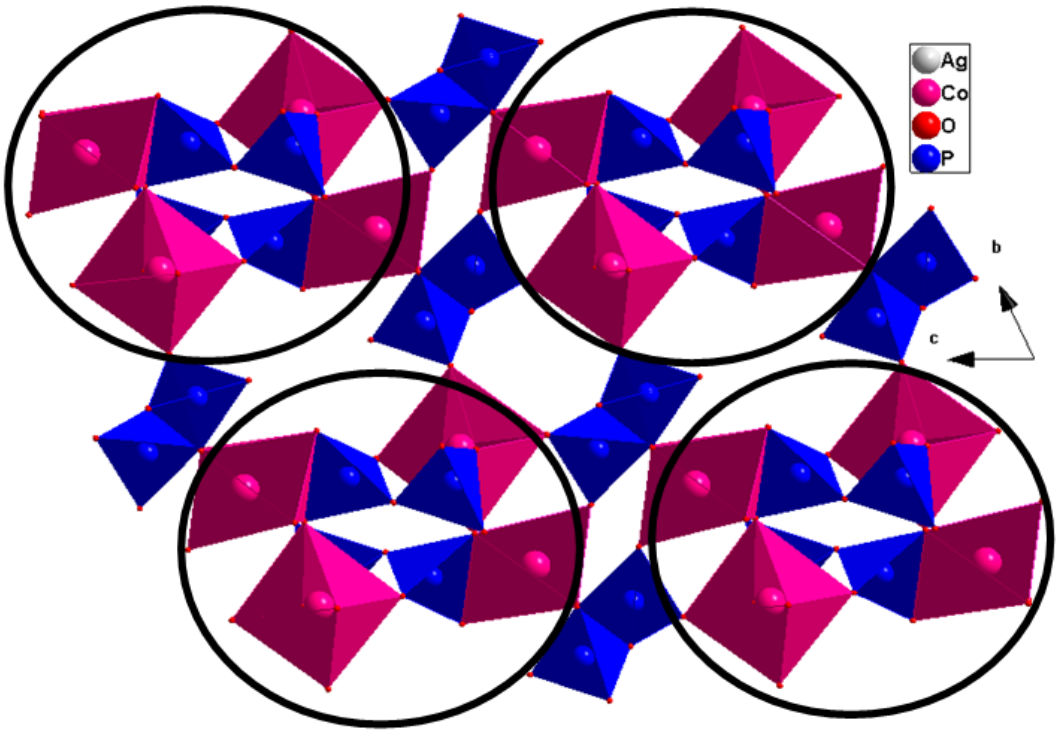

Figure 3. Projection in the *bc* plan showing junction between $Co_4P_4O_{28}$ units

The anionic framework shows different types of tunnels in *a*, *b* and *c* directions which located the silver ions (Fig. 4).

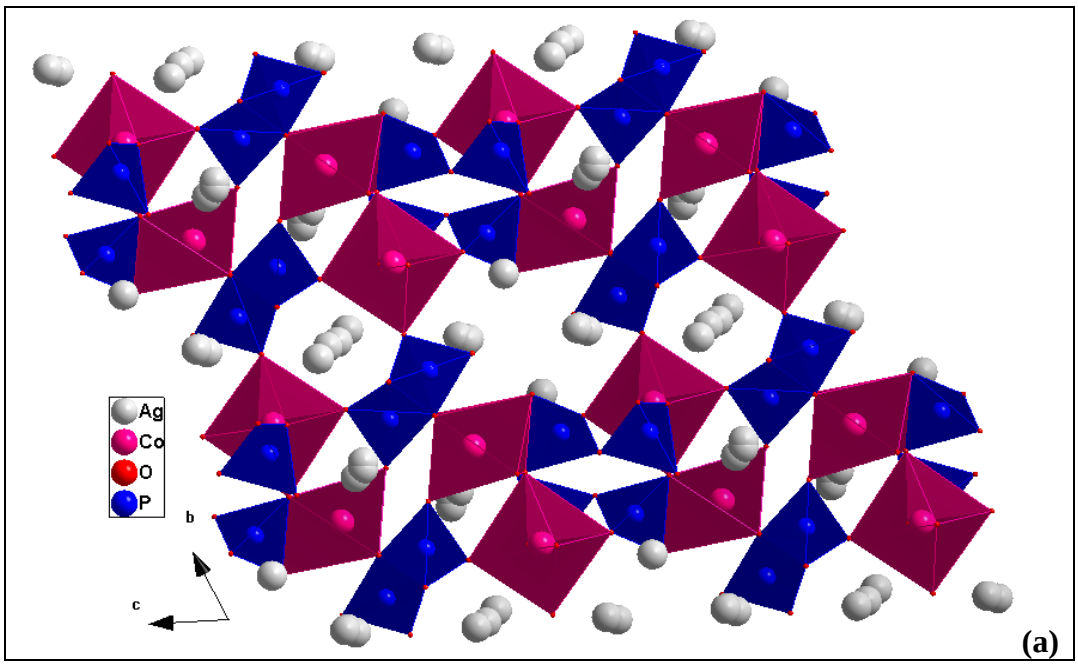

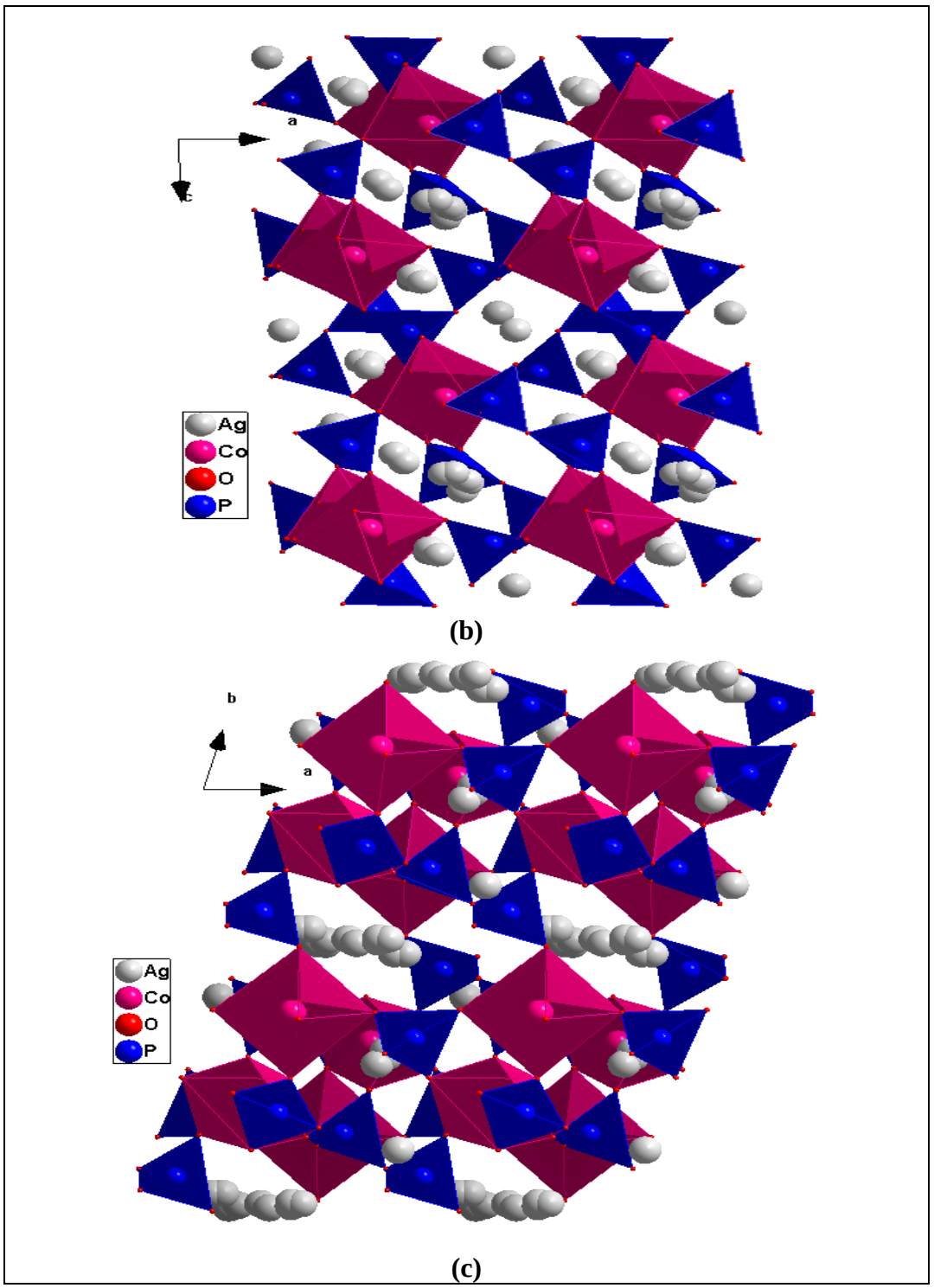

Figure 4. Projection along *a*, *b* and *c* directions showing different tunnels in $Ag_{3.68}Co_2(P_2O_7)_2$ structure.

3.3. Silver transport in $Ag_{3.68}Co_2(P_2O_7)_2$:

Silver transport pathways in $Ag_{3.68}Co_2(P_2O_7)_2$ are simulated using the Crystallographic Information Data file (CIF File) of the obtained structural data. Pathways are displayed like regions

enclosed by isosurfaces of constant |ΔV(Ag)| for a grid of hypothetical Ag positions covering the entire unit cell with a motion of 0.1 Å. The BVSE calculation results are described in figure 5.

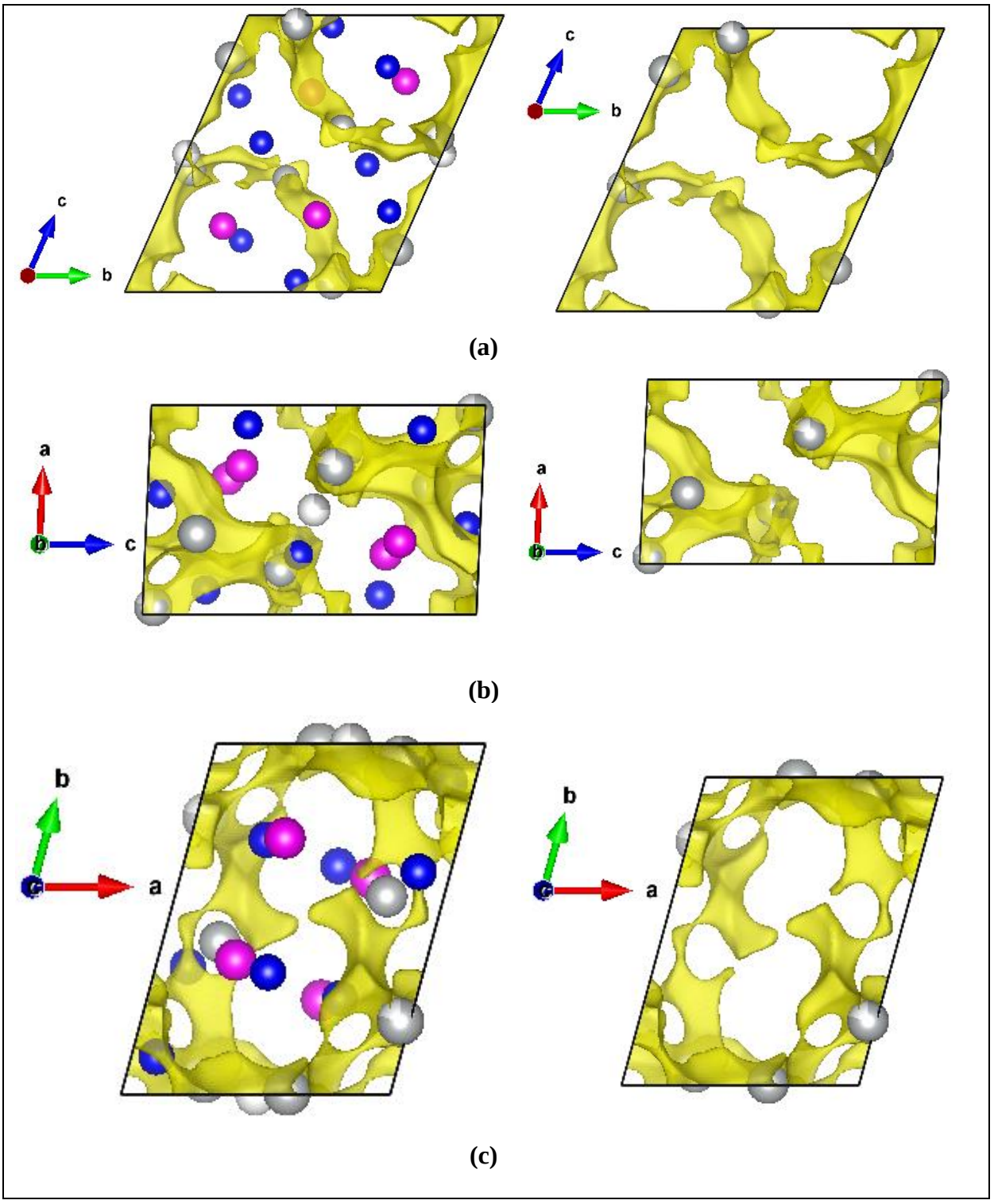

Figure 5. Bond-valence site energy depicted as landscapes (isovalue 1.7 eV above the E_{min}) for Ag^{+} mobility in $Ag_{3.68}Co_2(P_2O_7)_2$ projected in directions: a: (100); b: (010); & c: (001).

The equilibrium sites of the silver ions are marked as gray spheres which were the absolute minimum valences of Ag atoms in the structure. Yellow regions correspond to the low energies of silver interstitial sites which are most likely conduction pathways.

The BVSE simulation shows that, at the isovalue of |ΔV(Ag) |=1.3 u.v., the isosurfaces form continuous pathways (Fig. 6). It also indicates that pathways form at an activation energy about 1.7 eV in all dimensions at the same time. Thereby, comparing with other silver materials such as $Ag_4Co_7(AsO_4)_6$ (Ea=0.45 eV) [36] and similar diphosphates like $Na_{2.84}Ag_{1.16}Co_2(P_2O_7)_2$ (Ea=1.37 eV) [35], $Na_2CoP_2O_7$ (Ea=0.61 eV) [6], $Na_{1.14}K_{0.86}CoP_2O_7$ (Ea=1.34 eV) [7], the material should be moderate 3D ionic conductor.

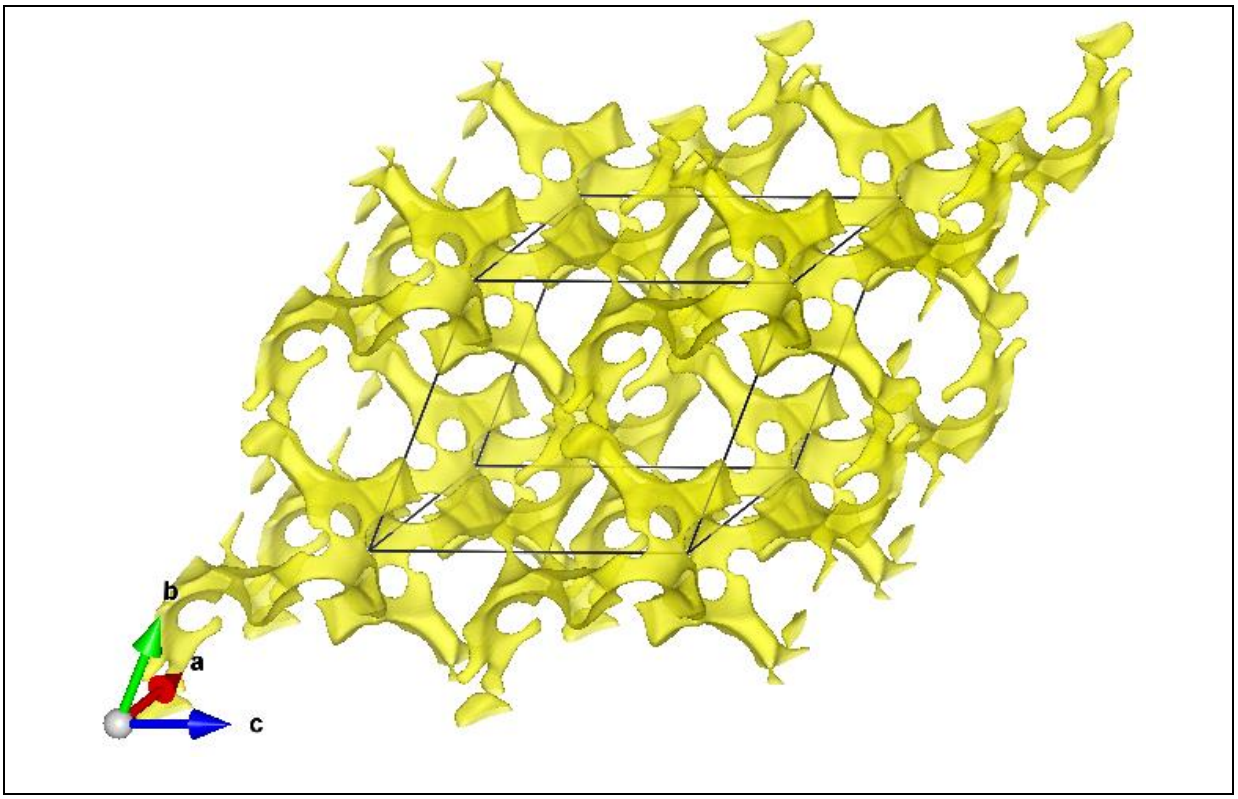

Figure 6. 3D pathways with bond valence mismatch of |ΔV(Ag) |=1.3 u.v (i.e. ~ 1.7 eV)

The obtained results are in good agreement with the structural data of the studied material. Indeed, structural study shows tunnels according to the three directions of unit cell (Fig. 7). In fact, along *a*-axis, two types of tunnels are shown, with decagonal and hexagonal forms, which minimum sections are 3.577 (5) Å and 3.842 (4) Å, respectively. Along *b* axis, the minimum section of the only one type of tunnel is relatively smaller, 2.829 (9) Å (Figure n). While the minimum tunnel section along *c* direction is 4.566 (8) Å measured between the oxygen atoms.

On the other hand, the agitation of silver cations and their partial occupations are factors that influence the ionic conduction.

Although the value of the activation energy is relatively high, electrical measurements will be interesting to know the electrical behavior of the title material. Indeed, the BVSE model considers only

the ionic conduction, so that electric conduction can occur, given the presence of two degrees of oxidation of cobalt (+II/+III).

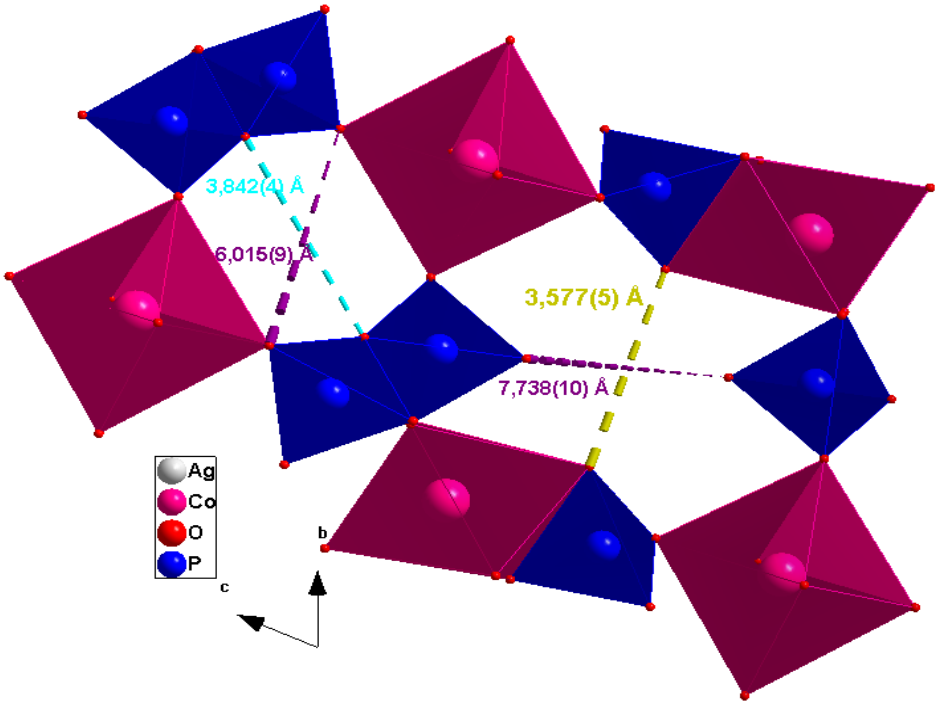

(a)

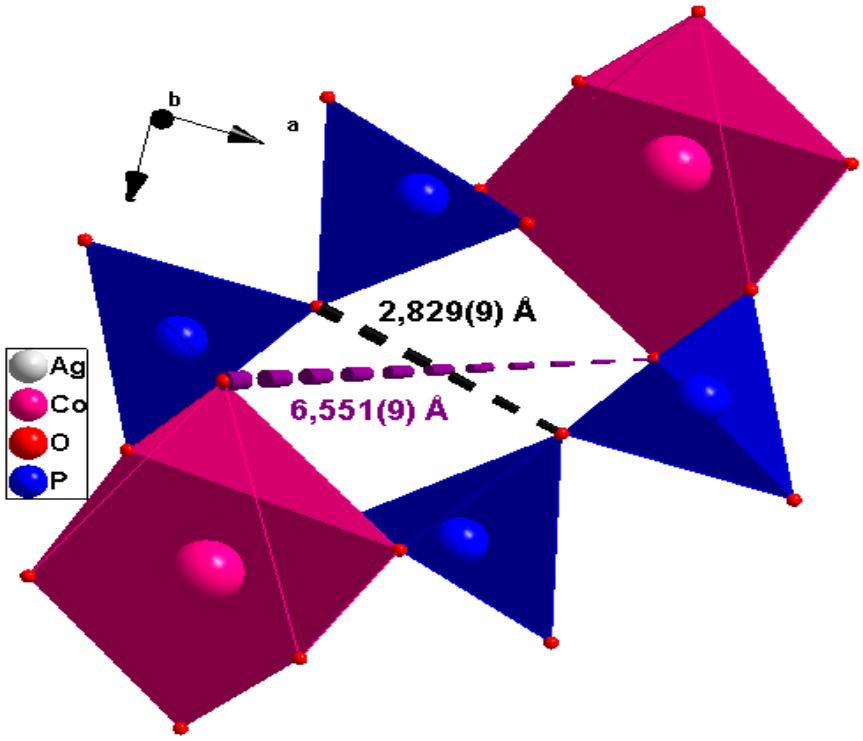

(b)

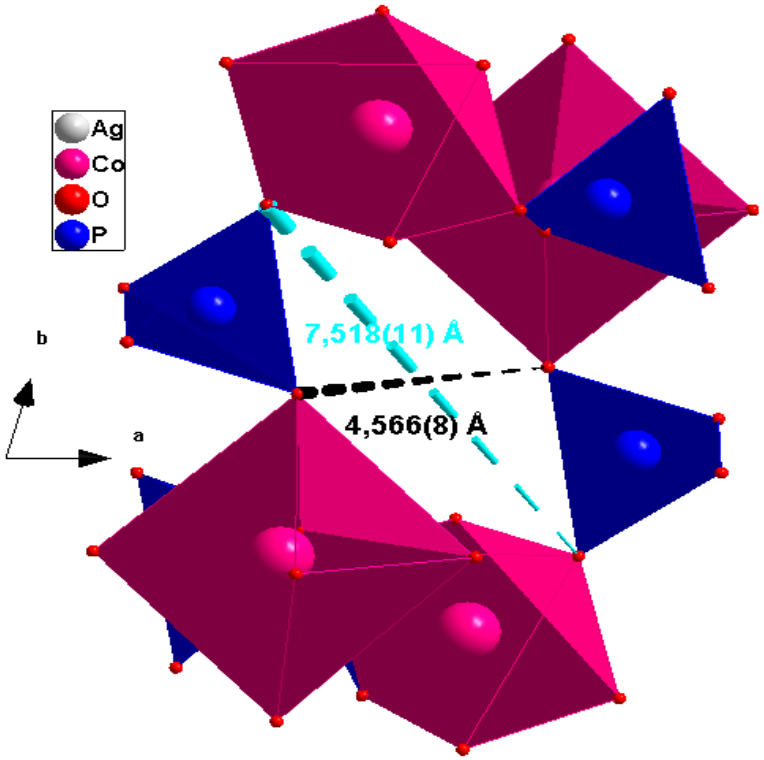

(c)

Figure 7. Dimensions sections of tunnels along *a:* (a) , *b:* (b) and *c*: (c) axes.

4. CONCLUSION

The $Ag_{3.68}Co_2(P_2O_7)_2$ material was synthesized by the dry route. This compound crystallizes in the triclinic system, space group P-1 with a = 6.521(4) Å, b = 9.623(6) Å, c = 10.969(7) Å, α = 64.23(2)˚, β = 80.14(3)˚ and γ = 72.10(2)˚. The anionic framework is formed by $Co_4P_4O_{28}$ units linked by diphosphate groups along *a*, *b* and *c* axes. It can be described as three 3D framework with two types of tunnels along *a* direction and only one tunnels type along [010] and [001] directions where the Ag^+ cations are located. The BVSE model is consistent with the structural study. It allowed us to model the conduction pathways of the silver ions; On the other hand, it shows that the material should be moderate three-dimensional conductor with activation energy of 1.7 eV. Beside the ionic conduction, electronic conduction is also possible due to the presence of two oxidation states of cobalt. The mixed conduction can be validated by electrical measurements in subsequent works.

ACKNOWLEDGEMENTS
The authors extend their appreciation to the Deanship of Scientific Research at King Khalid University for funding this work through research groups program under grant number R.G.P.1/25/38).
The authors gratefully acknowledge Prof. Maxim Avdeev (Australian Nuclear Science and Technology Organisation) for fruitful discussions.

SUPPORTING DATA

CIF file containing more details of the crystal structure was deposited in the Cambridge Crystallographic Data Centre (CCDC), 12 Union Road, Cambridge CB2 1EZ, UK; Fax: +44(0)1223-762911; email: deposit@ccdc.cam.ac.uk] (or at www.ccdc.cam.ac.uk/conts/retrieving.html) on quoting the deposit numbers CCDC1870084.

References

1. R. Ben Said, B. Louati, K. Guidara, *Ionics,* 20 (2014) 209-219.
2. M. Nagpure, K. N. Shinde, V. Kumar, O. M. Ntwaeaborwa, S. J. Dhoble, H. C. Swart, *J. Alloys Compd.*, 492 (2010) 384-388,**.**
3. J. G. Chen, L. Ang, C. Wang, Y. Wei, *J. Alloys Compd*., 478 (2009), 604-607.
4. T. Kanazawa, 52, Elsevier, Amsterdam, 1989, **«** Inorganic Phosphate Materials, Materials Science Monographs **»**.
5. B. Louati, F. Hlel and K. Guidara, *J. Alloys Compd*., 486 (2009) 299-303.
6. F. Sanz, C. Parada, J.M. Rojo, C. Ruiz-Valero, R. Saez-Puche, *J. Solid State Chem*., 145 (1999) 604-611.
7. R. Marzouki, Y. Ben Smida, A. Guesmi, S. Georges, Ismat H. Ali, S. Adams, M.F Zid, *Int. J. Electrochem. Sci.*, 13 (2018) *accepted doi: 10.20964/2018.12.75*
8. M. Sale, M. Avdeev, Z. Mohamed, C. D. Ling, P. Barpanda, *Dalton Trans*., 46 (2017), 6409-6416.
9. A. K. Padhi, K. 5. Nanjundaswamy, J. B. Goodenough, *J. Electrochem. Soc.*, 144(4), (1997) 1188-1194.
10. H. Y- P. Hong, *Mater. Res. Bull.*, 11 (1976) 173-182.
11. J. B. Goodenough, H. Y-P. Hong, J. A. Kafalas, *Mater. Res. Bull.*, 11, (1976) 203-220.
12. P. Barpanda, J. Lu, T. Ye, M. Kajiyama, S.C. Chung, N. Yabuuchi, S. Komaba, A. Yamada, *RSC Adv.*, 3 (2013) 3857-3860.
13. P. Barpanda, M. Avdeev, C.D. Ling, J. Lu, A. Yamada, *Inorg. Chem*., 52 (2013) 395-401.
14. SADABS: Area-Deatector Absorption Correction, Siemens Industrial Automation, Inc.: Madison, WI, 1996.
15. G.M. Sheldrick. *Acta Cryst*., A64 (2008) 112-122.
16. L.J. Farrugia, *J. Appl. Crystallogr*., 32 (1999) 837-838.
17. K. Brandenburg, M. Berndt (2001) Diamond Version 2.1. Crystal Impact. Bonn.
18. I.D. Brown (2002) The Chemical Bond in Inorganic Chemistry- The Bond Valence Model. IUCR Monographs on Crystallography. 12. Oxford University Press.
19. S. Adams (2003) softBV, University of Göttingen. Germany. http://www.softBV.net.
20. R. Marzouki, W. Frigui, A. Guesmi, M.F. Zid, A. Driss, Acta Cryst., E69 (2013) i65-i66.
21. R. Marzouki, A. Guesmi, A. Driss, Acta Cryst., C66, (2010) i95–i98
22. M. Sonni, R. Marzouki, M.F. Zid, A. Souilem, *Acta Cryst.*, E72, (2016) 833–837.
23. R. Marzouki, A. Guesmi, M.F. Zid, A. Driss, *Ann. Chim. Sci. Mat*., 38 (3-4) (2013) 117-129.
24. Y. Ben Smida, R. Marzouki, S. Georges, R. Kutteh, M. Avdeev, A. Guesmi, M. F. Zid, *J. Solid State Chem*., 239 (2016) 8-16.
25. Y. Ben Smida, R. Marzouki, A. Guesmi, S. Georges, M.F. Zid, *J. Solid State Chem*., 222 (2015) 132-139.
26. R. Nasri, R. Marzouki, S. Georges, S. Obbade, M. F. Zid, *Turk. J. Chem*., 42 (2018) 1251-1264.
27. S. Adams, R. Prasada Rao, *Phys. Status Solidi*, A 208 (2011) 1746-1753.
28. S. Adams, R. Prasada Rao, *Atom Indonesia,* 36 No.3 (2010) 95-104.
29. S. Marik, C. Nicollet, M. Channabasappa, S. Fourcade, A. Wattiaux, M. Duttine, R. Decourt, J.M. Bassat, O. Toulemonde, *Fuel Cells*, 17 (2017) No. 3, 353-358.

30. F. Hanic, Z. Zak, *J. Solid State Chem.*, 10 (1974) 12-19.
31. J. Angenault, J. C. Couturier, M. Quarton, F. Robert, *Eur. J. Solid State In. Chem.*, 32 (1995) 335-343.
32. F. Erragh, A. Boukhari, F. Abraham, B. Elouadi, *J. Solid State Chem.*, 152 (2000) 323-331.
33. R. Hoppe, S. Voigt, H. Glaum, J. Kissel, H. P. Muller, K. Bernet, *Less Common. J. Met*., 156 (1989) 105–122.
34. M. Nespolo, G. Ferraris, G. Ivaldi, R. Hoppe, *Acta Cryst*., B57 (2001) 652–664.
35. R. Marzouki, A. Guesmi, M.F. Zid, A.Driss, *Crystal Structure Theory and Applications, 1* (2013) 68-73.
36. R. Marzouki, A. Guesmi, S. Georges, M. F. Zid, A. Driss, *J. Alloys Compd*., 586 (2014) 74-79.